

NOVEL TERAHERTZ PHOTOCONDUCTIVE ANTENNAS

**Masahiko Tani,¹ Yuichi Hirota,¹ Christopher T. Que,¹
Shigehisa Tanaka,² Ryo Hattori,³ Mariko Yamaguchi,¹
Seizi Nishizawa⁴ and Masanori Hangyo¹**

¹ *Institute of Laser Engineering, Osaka University
2-6 Yamadaoka, Suita, Osaka 565-0871, Japan
E-mail : tani@ile.osaka-u.ac.jp*

² *Central Research Laboratory, Hitachi Ltd.,
1-280, Higashi-koigakubo, Kokubunji-shi, Tokyo 185-8601, Japan*

³ *Advanced Technology R&D Center, Mitsubishi Electric Corp.
8-1-1 Tsukaguchi-honmachi, Amagasaki 661-8661, Japan*

⁴ *Aispec: Advanced Infrared Spectroscopy Co.,Ltd.
3-17-16 Sen-nin-cho, Hachioji, Tokyo 193-0835, Japan*

Abstract

The photoconductive (PC) antenna is a key device for the recent terahertz (THz) photonics based on laser-pumped generation and detection of THz radiation. In this paper we report on two new types of PC antennas: the Schottky PC antenna and the multi-contacts PC antenna. The former one is able to detect THz radiation intensity without the time-delay scan and useful for applications where spectroscopic information is not important, such as the THz intensity imaging. The latter one is useful for the polarization sensitive THz spectroscopy, such as the THz ellipsometry. The characteristic features of these new types of PC antennas are studied by using a THz time-domain spectroscopy system.

Key Words: Terahertz radiation, photoconductive antennas, Schottky contact, rectification effect, multi-contacts, polarization modulation

1. Introduction

Since the first demonstration of generation and detection of pulsed THz radiation with photoconductive (PC) antennas in early 80s [1], the PC antenna has been one of the most important devices for terahertz photonics, even after the other THz-pulse emitting and detecting devices, such as the electro-optic (EO) emitter and detectors, were developed. It still has superiority in the efficiency

and stability. (i) It has a high efficiency in conversion from the optical-pump power to THz-emission power. A 10 mW average power with a standard mode-locked Ti: sapphire laser oscillator (corresponding to a peak power about 1 kW) is enough to pump or trigger a PC antenna, while other emitting devices such as EO crystals or semiconductor surfaces require an order of magnitude higher pump power. (ii) The photoconductive detection is relatively stable against optical and thermal noise, while the EO sampling detection is very sensitive to such noises. With these advantages, PC antennas are the most widely used as the emitter and detector in the so-called “Terahertz-time-domain spectroscopy (THz-TDS)”, where pulsed THz radiation is generated by excitation of an emitter with femtosecond laser and the waveform of the THz radiation (transmitted through a sample) is measured with a sampling detector scanning the time-delay. A high signal-to-noise ratio (SNR) is obtained in the absorption and dispersion spectra with the THz-TDS system using a pair of PC antennas as the emitter and detector: the dynamic range, defined by the ratio of the maximum level of the power spectrum and the noise level, is typically on the order of 10^6 for a standard THz-TDS system with a measurement time of a few minutes (for the case of the slow-delay line).

We firstly outline the basic principle of generation and detection of THz radiation with PC antennas in the next section. Then, in the following sections we describe two novel types of PC antennas: one is a PC antenna with a Schottky contact (Schottky PC antenna), and the other is a PC antenna with multi-contact (four-contact PC antenna). The Schottky PC antenna is aimed to detect the intensity of THz pulsed radiation without the time-delay scan using the rectification effect of the Schottky contact although the spectral information is lost through the rectification process. Such a Schottky PC antenna is useful for applications, such as the THz intensity imaging, where the THz spectral information is not required. The multi-contact PC antenna is aimed to generate THz radiation whose polarization is alternately switched between the two orthogonal states. Such a polarization-modulated THz emitter is useful, for example, in THz ellipsometry, where the ratio of the orthogonal polarization components need to be measured with a high SNR. In addition, when it is used as a detector, the two polarization field components of THz radiation is detected simultaneously, which is also useful for THz ellipsometry and other polarization sensitive measurements.

2. Basic characteristics of photoconductive antennas

It is well known that the radiated electric field from a point source is proportional to the time derivative of the point current in far-field (the dipole approximation). As a simple extension of this principle, the electric field from a distributed current is given by the volume integration of the time-derivative of the current density, $j(\mathbf{r}', t')$, which is defined at a point, \mathbf{r}' , and time, t' . The THz electric field emitted from a PC antenna is thus expressed by the following equation [2]:

$$E_{THz}(\mathbf{r}, t) = -\frac{1}{4\pi\epsilon c^2} \int_{+antenna}^{gap} \left[\frac{\partial j_{PC}(\mathbf{r}', t')}{\partial t'} \right]_{t'=t_r} \frac{\sin \theta}{|\mathbf{r} - \mathbf{r}'|} d^3x' \tag{1}$$

Here, the THz electric field, $E_{THz}(\mathbf{r}, t)$, is given at the observation point, \mathbf{r} , and the observation time, t . ϵ and c are the dielectric constant of the medium (for the vacuum $\epsilon=\epsilon_0$) and the speed of light, respectively. $j_{PC}(\mathbf{r}, t)$ is the photoconductive current density on the PC gap or the PC antenna. The time-derivative is taken at the retarded time, defined by $t_r = t - |\mathbf{r} - \mathbf{r}'|/c$. θ is the angle between the current direction and observation direction. This is a general equation for an emitting antenna, from which the amplitude and phase of the radiated electric field at a point and time, $E_{THz}(\mathbf{r}, t)$, is calculated unambiguously. The radiation pattern of an antenna is determined by the interference between the field components emitted from different points on the antenna. Therefore, the shape and dimension of the PC antenna determines the THz radiation pattern.

The current in a PC antenna is modulated by a femtosecond laser pulse incident on the PC gap through a change of the photoconductance, while the current in an ordinary microwave antenna is modulated electrically. Because of the parasitic capacitance or inductance it is not possible to modulate the current electrically at THz frequencies. On the other hand, by the use of femtosecond laser pulses, it is possible to create a sub-picosecond photoconductive transient current in a biased PC antenna and generate THz pulsed radiation according to Eq. (1).

When a constant bias field, E_{bias} , is applied to the PC gap, the current density, $j_{PC}(\mathbf{r}, t)$, in the PC gap is given by the following equation:

$$j_{PC}(t) = \frac{\sigma(t)E_{bias}}{\frac{\sigma(t)Z_0}{1+n_d} + 1} \tag{2}$$

Here, $\sigma(t)$ is the conductivity, Z_0 is the characteristic impedance of vacuum, and n_d

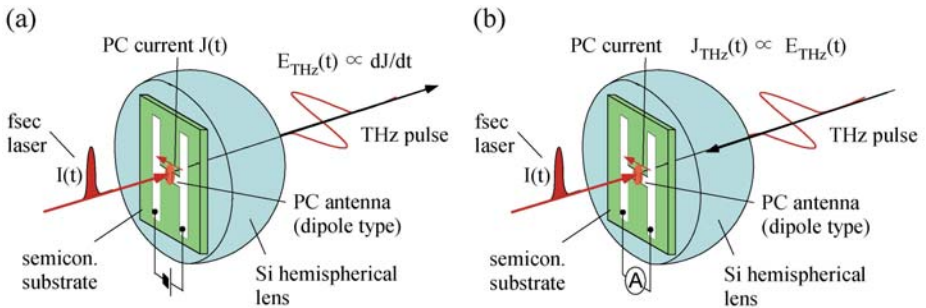


Fig. 1. (a) A PC emitter antenna and (b) a PC detector antenna mounted on a hemispherical substrate lens.

is the refractive index of the substrate. The numerator is corresponding to the ordinary ohmic law and the denominator is corresponding to the saturation effect due to the field screening by charged carriers. The conductivity $\sigma(t)$ is modulated by the pump laser: the rise time is equal to the width of the pump pulse and the decay is determined by the carrier lifetime in the substrate semiconductor, which is usually longer than the pump pulse width.

The schematic illustration of an emitting PC antenna is shown in Fig. 1(a). The PC antenna consists of a microstrip antenna with a PC gap locating at the center of a coplanar transmission line and a semiconductor substrate with a short carrier lifetime, such as the low-temperature grown GaAs (LT-GaAs) [3]. The biased PC gap is illuminated to generate sub-picosecond current transient in the antenna, which is usually contacted with a hemi-spherical or hyper hemispherical substrate lens made with high resistivity silicon for a better coupling of THz radiation to the free space.

For detection of the pulsed THz radiation, the same type of PC antenna is used (Fig. 1(b)). The detector PC antenna is activated with a trigger femtosecond laser pulse, which is separated from the pump femtosecond laser. When THz radiation is incident on the detector PC antenna synchronously with the trigger laser pulse, the photoexcited carriers are accelerated by the THz field giving rise to a signal current in the detector PC antenna. The averaged signal current, $i_{THz}(\tau)$, detected with the PC antenna for a relative time delay, τ , is given by the convolution of the transient photoconductance, $G(t)$, of the detector PC antenna and the incident THz field, $E_{THz}(t)$:

$$i_{THz}(\tau) \propto \int G(t - \tau) E_{THz}(t) dt \quad (3)$$

If the photoconductive response function $G(t)$ is sharp enough compared to the duration of THz radiation pulse $E_{THz}(t)$, as the case of an extremely short carrier lifetime in the substrate, so that $G(t)$ is approximated as a delta function, the signal $i_{THz}(\tau)$ is proportional to the THz electric field waveform $E_{THz}(\tau)$. If $G(t)$ is

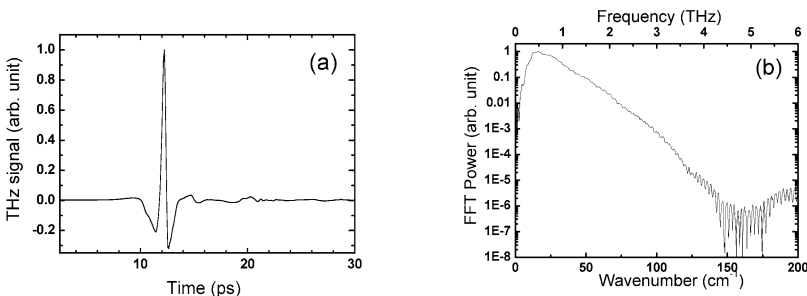


Fig. 2. (a) The THz signal waveform detected with a PC antenna. (b) The power spectrum obtained by Fourier transforming

the waveform in Fig.2 (a).

approximated with a step function, as the case with a long carrier lifetime, $i_{THz}(\tau)$ is proportional to the time-integrated waveform of $E_{THz}(\tau)$. This photoconductive sampling scheme (a kind of pump-probe measurement) is very unique and distinguish the PC antenna from other conventional detectors, such as the pyroelectric detector or bolometer, who detects the radiation power. By Fourier transforming the time domain signal, $i_{THz}(\tau)$, we can obtain the amplitude and phase spectra of the THz radiation.

Since the photoconductive signal current is usually very weak (on the order of pA~nA), it is detected with a set of a current amplifier and lock-in amplifier modulating the pump laser or the bias on the emitter PC antenna. To measure the time-domain waveform, $i_{THz}(\tau)$, the relative time-delay between the pump and trigger laser pulse is scanned by using an automatic translation stage equipped with an optical reflector. A typical THz signal waveform and its Fourier transformed power spectrum are shown in Fig.2(a) and (b), respectively. A dynamic range, which is defined by the ratio of the spectrum peak level and noise floor, of the order of 10^6 is easily achieved with a single scan for a few minutes. The frequency resolution, $\delta\nu$, is determined by the inverse of the scanned time window, $\Delta T(=1/\delta\nu)$. The nominal measurement bandwidth, ν_{max} , is limited by the sampling step in the time-delay, $\Delta\tau$, and given by $\nu_{max} = 1/(2\Delta\tau)$. The actual bandwidth of the measurement system is mainly determined by the pulse width of the femtosecond laser used for the pump and trigger. The absorption due to optical phonons in the GaAs substrate (thickness 0.3~0.4 mm) significantly reduces the frequency components above 3THz. The water vapor absorption also becomes significant above 1 THz frequencies range, which can be reduced by filling the THz beam paths with dry air or nitrogen gas.

When this THz generation and detection system is applied for spectroscopy, we measure the time-domain THz signal with and without a sample inserted in the THz beam path. From the ratio of the complex Fourier transformed spectra (the amplitude and phase spectra) for the sample and reference (without sample), we can obtain the absorption and dispersion spectra of the sample. This method of spectroscopy is called "THz time-domain spectroscopy (THz-TDS)." The readers who are familiar with the Fourier transform spectroscopy might have noticed the similarity between the THz-TDS and the Fourier transform spectroscopy. The time-domain signal waveform in THz-TDS corresponds to the interferogram in Fourier transform spectroscopy. However, the interferogram in the ordinary Fourier transform spectroscopy only contains the intensity spectrum information and neither phase information nor dispersion spectrum is obtained [4].

For more detailed information on the characteristics of PC antennas and THz-TDS, readers are recommended to refer to the references [5-8].

3. Photoconductive antenna with Schottky contact

Schottky barrier diodes are often used to detect microwave intensity through the rectification effect for the alternating field. The ultimate bandwidth of the Schottky barrier diode is very broad, extending to THz frequencies,

although the actual bandwidth is limited by the contact capacitance and other peripheral, parasitic, capacitances. With a careful design of the contact (such as a point contact with a metal tip on n-type GaAs), Schottky barrier diode can detect THz radiation [9]. However, ordinary Schottky diodes are not suitable for detection of pulsed THz radiation (~ 1 ps) generated by excitation of a PC antenna (or other THz emitting devices) with femtosecond laser because they also detect continuous thermal background radiation, whose power is comparable or higher than the average power of the pulsed THz waves. This problem is alleviated if the Schottky barrier diodes can be photo-activated by the same laser pulses used to pump the emitter. In other words, if a PC antenna activated by laser pulses can rectify the THz signal within a limited time-window, rejecting most of the thermal radiation, we can detect the intensity of the pulsed THz radiation without the time-delay scan.

In this section we describe a new type of PC antenna, that is, the Schottky PC antenna, which rectifies the photoconductive THz signal and is able to detect THz intensity without the optical delay scan [10]. An ordinary PC antenna samples the THz electric field gated with an optical short pulse synchronized with the THz radiation pulse, and the signal corresponding to the THz waveform is measured with varying the optical delay between the THz pulse and the gating pulse, as described by Eq.(3). On the other hand, the Schottky PC antenna rectifies the THz signal during the photocarriers excited with an optical gate pulse and give rise to a dc signal which is corresponding to the integration of positive (or negative) THz field without optical delay scan.

We fabricated an asymmetric PC antenna on a semi-insulating GaAs (SI-GaAs) substrate, as illustrated in Fig. 3. The PC antenna consists of a coplanar stripline (~ 8 mm) with a $100 \mu\text{m}$ separation and a triangular stub ($\sim 50 \mu\text{m}$) at the center of one of the stripline made of aluminum (the other line was made of an alloy of Ni, Ge, and Au to make an Ohmic contact). The width of the striplines was about $10 \mu\text{m}$. THz radiation was generated by another PC antenna fabricated on LT-GaAs and detected by the Schottky PC antenna, each of which was pumped

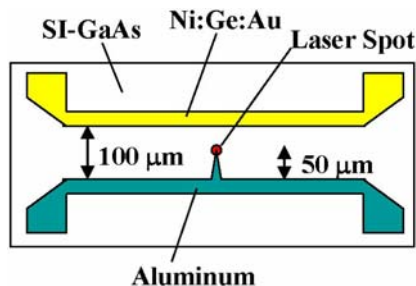


Fig. 3. Structure of the asymmetric PC antenna with a Schottky contact.

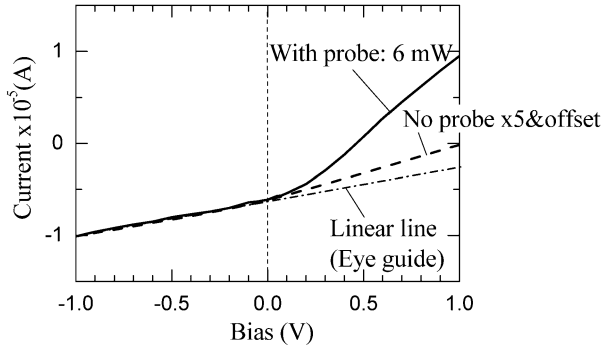


Fig. 4. dc I-V characteristics of the asymmetric PC antenna.

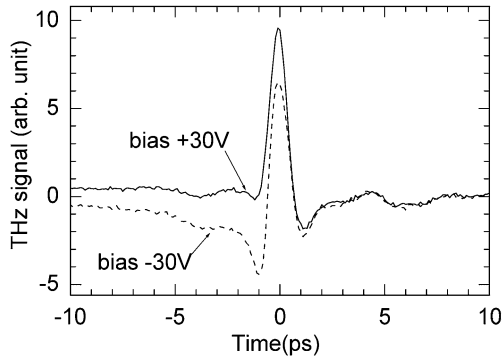


Fig. 5. The THz waveforms detected by the Schottky PC antenna for the +30-V and -30-V bias.

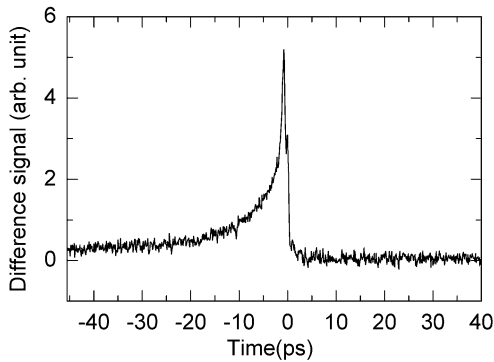


Fig. 6. The difference of the two waveforms in Fig.5.

and probed with a femtosecond laser ($\lambda \sim 790$ nm, $\delta t < 100$ fs, 75 MHz). The pump and probe laser power was 50 mW and 7 mW, respectively. The probe laser was focused near the tip of the triangular Schottky contact of the PC antenna by an objective lens ($\times 50$) to a spot size of around 10 μ m. The pump laser was modulated at 2 kHz with a mechanical chopper. The detected current signal was amplified with a set of current amplifier and lock-in amplifier.

Figure 4 shows the dc I-V characteristics of the PC gap, measured with a 6 mW probe laser irradiated on the gap (solid line in the figure) and without the probe laser (dashed line in the figure). The latter (the dark current) was multiplied by a factor of 5 and offset to be compared with the photocurrent. The figure shows a similar I-V characteristics with that of a typical Schottky diode, that is, the asymmetric conductance for the forward (the ohmic contact is positively biased) and reverse bias field. The asymmetry is more pronounced for the photoconductance than for the dark conductance.

Figure 5 shows the THz time-domain waveforms, detected with the Schottky PC antenna, for the emitter biases of +30-V and -30-V. The polarity of the signal for the -30-V bias was reversed for comparison with the +30-V signal. It was confirmed from a separate experiment that in using an ordinary PC antenna detector the THz signal from the PC antenna emitter in reverse bias is identical to that of its forward bias except the polarity. Therefore, if there is no rectification effect in the asymmetric PC antenna, we should observe two THz waveforms identical in amplitude and shape for +30-V and -30-V bias. However, the two waveforms are different wherein the forward-bias-waveform (+30V) shows a higher positive peak and smaller negative signals at time $\tau < 0$ compared to the reverse-bias-waveform (-30 V). This result is explained by the rectification effect on the THz current by the Schottky barrier at the interface of the metal contact and the semiconductor substrate.

As described in the previous section, the THz photocurrent, $i_{THz}(\tau)$, at a time-delay τ is proportional to the convolution of the transient conductance, $G(t)$, of the PC gap, and the THz field on the detector (Eq. (3)). The photoconductance $G(t)$ of the Schottky PC antenna depends not only on the carrier density, $n(t)$, but also on the field strength and polarity. The rectified signal, $i_{rec}(\tau)$, is given by adding the signals of the THz radiation from the forward-bias, $E^{(+)}(t) = E(t)$, and that from the reverse-bias, $E^{(-)} = -E(t)$:

$$i_{rec}(\tau) = i_{THz}^{(+)}(\tau) + i_{THz}^{(-)}(\tau) \quad (4)$$

$$\propto \int G(t - \tau) E^{(+)}(t) dt + \int G(t - \tau) E^{(-)}(t) dt \quad (5)$$

$$= (S^{+} - S^{-}) \int n(t - \tau) |E(t)| dt \quad (6)$$

In Eq. (6), we assumed that the conductance $G(t)$ only depends on the carrier density, $n(t)$, and the polarity of the field (not on the field strength). S^{+} and S^{-} are the proportionality constants for the positive and negative fields, respectively. If the photoconductance is symmetric in both fields, $i_{rec}(\tau)$ vanishes because $S^{+} - S^{-} = 0$. However, when the photoconductance is asymmetric, $i_{rec}(\tau)$ gives the

rectified signal because $S^+ - S^- \neq 0$. Figure 6 shows the rectified THz signal given by Eq. (4) (the difference between the waveforms shown in Fig. 5). It shows a sharp rise at the zero time-delay and a slow decay toward the negative time-delay.

The decay characteristics in the rectified THz signal is reflecting the photo-carrier decay in the SI-GaAs substrate. If the characteristic time duration of the THz radiation pulse is much shorter than the carrier decay time, Eq. (6) gives a function proportional to $n(-\tau)$ which is characterized by a sharp rise due to the optical pulse excitation and subsequent slow carrier decay toward the negative time $(-\tau)$.

To verify the nonlinear signal is not from the asymmetric geometrical effect of the antenna, we also made a symmetric dipole-type antenna on LT-GaAs substrate, one of its contacts was made of aluminum and the other was made of AuGe/Au alloy. Although the rectified signal in the symmetric Schottky PC antenna was relatively small, probably due to the short carrier lifetime in LT-GaAs (~ 0.5 ps), the result was similar to that observed for the asymmetric Schottky PC antenna on SI-GaAs substrate.

The SNR of the Schottky PC antenna with SI-GaAs substrate was poor because of the thermal noise from the long-lived photocarriers. By optimizing the carrier lifetime in the GaAs substrate, the SNR is expected to improve.

Schottky PC antennas are useful for many applications, such as THz intensity imaging, since they can detect THz radiation intensity without the time-delay scan when used with an optical gate pulse of an appropriate length (~ 10 ps), enabling a quick THz intensity imaging.

4. Four-contact photoconductive emitter

In this section we describe a four-contact PC antenna [11], which is another new type of PC antenna. The four-contact PC antenna can be used to generate THz radiation whose polarization is alternately switched between two orthogonal directions by rotating the bias. When it is used as a detector in the THz time-domain measurement, it is also possible to determine the amplitude and the polarization direction simultaneously by detecting the photoconductive THz signal currents from the two pairs of contacts. Circular polarization modulation of THz radiation is also possible by using a $\pi/2$ phase retardation upon the internal total-reflection at a Si-air interface.

Before we describe our four-contact PC antenna and its results, let us summarize the attempts which have been done related to the polarization modulation and polarization sensitive detection of THz radiation. Chen and Zhang [12] successfully demonstrated a polarization modulation of THz radiation generated by optical rectification in a (110)-cut ZnTe crystal by rotating the polarization direction of the pump femtosecond laser. Shimano *et al* [13] reported a polarization modulation scheme using an electro-optic THz emitter (a ZnTe

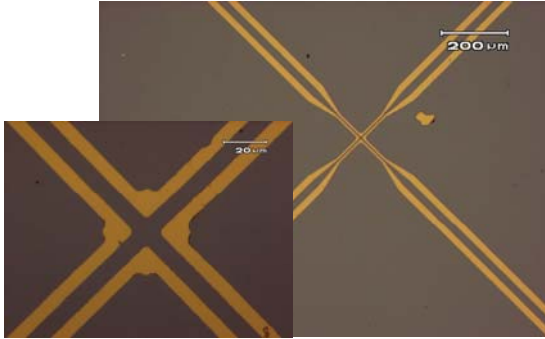


Fig. 7. A microscope view of the four-contact PC antenna. The magnified view of the center part is shown on the lower left.

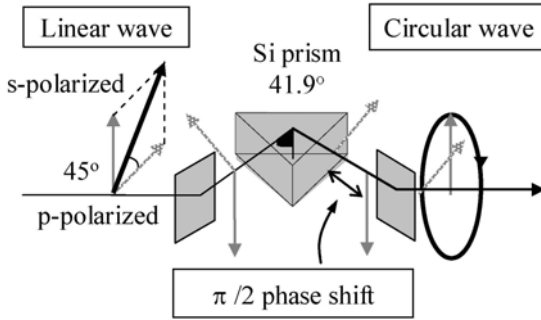


Fig. 8. Setup for the linear-to-circularly polarized THz wave conversion using the total reflection in the Si prism.

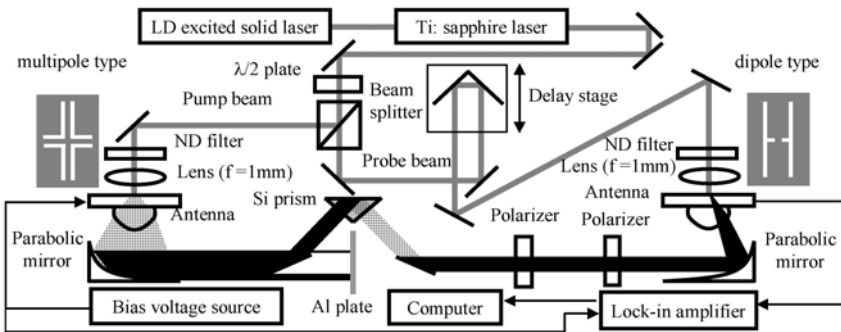


Fig. 9. The experimental setup for the generation and detection of circularly polarized THz radiation modulated with the four-contact PC antenna and the Si prism.

crystal) and an interferometer, by which one of the two orthogonally polarized THz radiation pulses was phase-retarded and the polarization state of the combined THz beam was modulated. However, with this method the ellipticity spectrum of such a broadband THz radiation can not be flat but periodic with the frequency because the phase retardation depends not only on the path difference in the interferometer but also the frequency of the THz radiation. Castro-Camus [14] reported a polarization sensitive PC detector, which has a three terminal contact to detect the orthogonal polarization components of the THz radiation simultaneously.

We fabricated a cross-shaped PC antenna, which has four metal contacts (as shown in Fig. 7), on an LT-GaAs substrate by a standard photolithographic and chemical etching method. By applying a bias voltage to the two adjacent electrodes with the other two is grounded, the bias electric field in the PC gap is directed to $+45^\circ$ or -45° from the horizontal axis. When a short pulse light (pump beam) is irradiated to the biased PC gap, the transient photocurrent generates THz radiation which is linearly polarized in the direction of the bias field. By rotating the bias voltages by 90° , we can generate THz radiation with the same amplitude but with the polarization orthogonal to the previous one. Since the bias voltage is switched easily and quickly by using an appropriate electronic circuit, the polarization direction of THz radiation is alternated between the $+45^\circ$ and -45° direction at a rate more than several kHz.

These linearly polarized waves are converted to circularly polarized waves by using the total reflection within a high-resistivity Si prism (see Fig. 8): the *s*-polarized component of electromagnetic waves are phase-retarded against *p*-polarized one by the total reflection and its phase-shift depends on the reflection angle. The internal reflection angle of the Si prism is designed to give rise to a $\pi/2$ phase-shift so that the linearly polarized waves at $+45^\circ$ becomes left-handed circularly polarized waves, and, in the same way, the ones at -45° become right-handed circularly polarized waves. This linear-to-circular-polarization conversion method is effective for a broadband THz pulsed waves because the total reflection phase-shift is independent of the wavelength due to the flat dispersion of Si in the THz frequency range. In this way, the combination of a four-contact PC antenna and a Si prism enables us to build a broadband, circularly polarized THz wave source and modulator.

We used a mode-locked Ti: sapphire laser operated at 80 MHz ($\lambda \sim 770$ nm, $\delta\lambda \sim 10$ nm) as the light source. A polarization beam splitter split the laser beam into a pump beam and a probe beam. The power balance between the pump and probe beam was controlled by rotating a half waveplate before the polarization beam splitter (see Fig. 9). The pump beam with an averaged power of 20 mW was focused on the gap of the four-contact PC emitter. The bias voltages on the antenna were modulated at 33 kHz. For generation of THz radiation with the polarization axis directed to $+45^\circ$, the antenna contacts at the top, right, left and bottom shown in Fig. 7 were biased to 0 V, 0 V, 30 V and 30V, respectively, and in the case of -45° polarization, these electrode were biased to 30 V, 0 V, 30 V and 0V, respectively (the bias field was rotated by 90°). Thus, the polarization of

the emitted THz radiation was alternated between $+45^\circ$ and -45° directions as the bias was modulated.

For detection, the THz radiation was focused on a dipole-type PC antenna by a pair of parabolic mirrors. The probe beam of 20 mW was focused on the gap of the detector antenna for the photoconductive sampling of the THz field. Since the direction of the detector PC antenna was oriented to horizontal direction, the polarization components of the THz field at 0 or 180° from the horizontal axis are detected. By moving the optical-delay-line and detecting the photoconductive signal step by step, the time domain THz waveforms were measured.

Since we used a lock-in amplifier synchronized with the alternating bias on the emitter antenna, the detected signal was the difference of the amplitude between the two switched waves. Moreover, by additionally modulating the pump beam with a mechanical chopper at 3.3 kHz and using this modulation frequency as the reference for the lock-in amplifier we were able to detect the average of the amplitude of the two switched waves: since the amplifier detects the difference of the signals with the pump and without the pump, while the bias was modulated at a

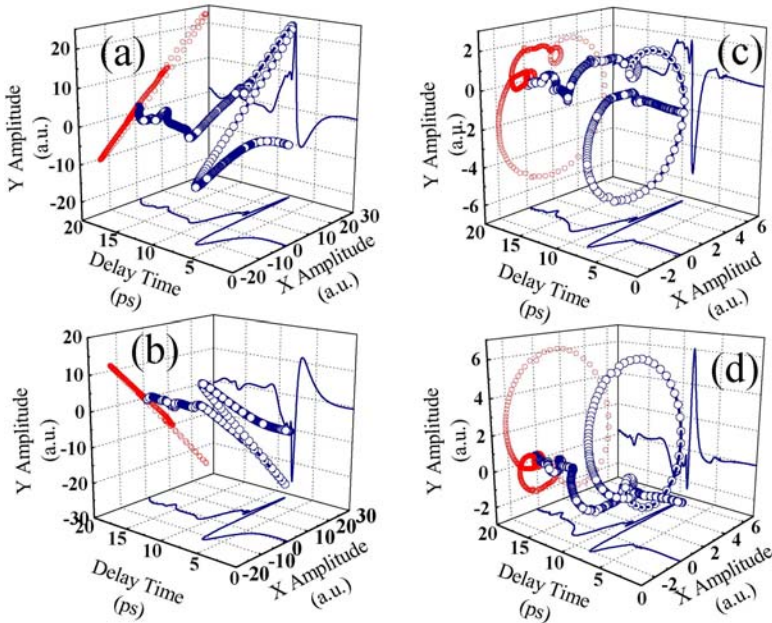


Fig. 10. The trajectories of the electric field vectors for the (a) $+45^\circ$ -linear wave, (b) the -45° -linear wave, (c) the left-circularly-modulated wave, and (d) the right-circularly-modulated wave.

much higher frequency (33 kHz), the average of the amplitude of the two switched waves was detected. By rotating the wire-gird polarizer inserted between the two parabolic mirrors, we detected the polarized components of the THz wave in the $+45^\circ$ and -45° directions. From the difference and average signals we can construct the trajectories of the THz electric field vectors in time and space, that is, the THz waveform presented in the three dimensional space which consists of the time axis and the polarization plane, for the two switched waves.

The trajectory of the THz electric fields for the $+45^\circ$ and -45° directional bias voltage are shown in Fig. 10 (a) and (b), respectively. In Fig.11, the frequency dependence of the ellipticities (the ellipticity spectra) of the two linearly polarized THz waves are shown by the solid and open squares, respectively. In these figures, we could see that each THz wave is almost linearly polarized in the corresponding bias direction. However, the ellipticities of the $\pm 45^\circ$ -waves were not exactly zero (corresponding the perfect linear polarization), but have values between -0.05 to $+0.1$, indicating slightly poor linear polarization.

The trajectories and the ellipticity spectra of the THz waves transmitted through the Si prism with the bias voltage modulation in directions to $+45^\circ$ and -45° are shown in Fig. 10 (c), (d) and Fig. 11 (the solid and open circles),

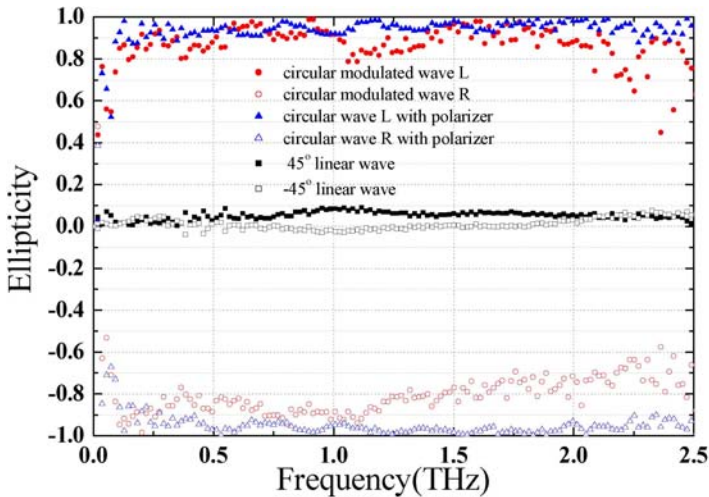


Fig. 11. The ellipticities of the orthogonal two linearly polarized THz waves (solid and open squares), those of the left and right circularly polarized THz waves with a linear- polarizer (solid and open triangles), and those of the left and right circularly polarized components of the modulated THz waves without a

linear-polarizer (solid and open circles), respectively. In these results, we could see that two switched waves were nearly left and right-handed circular waves, and that we succeeded to generate the circularly modulated broadband THz radiation from 0.1 to 2.5 THz. However, the ellipticities of the modulated waves were not exactly 1.0 (that corresponds to a perfect left-handed circular wave) or -1.0 (a right-handed one), indicating the circular polarization of the modulated waves was not perfect.

When THz radiation was prepared in a linear polarization state at $+45^\circ$ or -45° by using a wire-grid THz polarizer and transmitted through the Si prism, we observed a nearly perfect circular polarization (the ellipticity very close to $+1$ or -1) as indicated by the solid and open triangles in Fig. 11. Therefore, the main reason of the imperfect circular polarization is attributed to the distortion from the linear polarization of THz radiation emitted by the four-contact PC antenna.

There are several factors which may cause the distortion of the polarization of THz radiation from the PC antenna: the spatial inhomogeneity of the photoelectric property of the photoconductive substrate (LT-GaAs), the asymmetric or inhomogeneous distribution of the pump beam intensity and the deviation of the bias field distribution from the ideal symmetry, such as due to an imperfect patterning of the contact electrodes. When an inhomogeneous pump beam is incident on the PC gap, or the pump beam is incident off-centered on the PC gap, with an inhomogeneous bias electric field distribution, the polarization of the emitted THz radiation will be significantly distorted from the linear polarization.

We believe our circular-polarization modulation method using the bias modulation on a four-contact PC antenna and the total reflection in a Si prism is useful when it is applied to the VCD spectroscopy for chiral molecules in the THz frequency range. The four-contact PC antenna alone is also useful for the THz ellipsometry [15]. If it is used to generate linearly polarized THz radiation with its polarization direction alternated by the bias switching and another four-contact PC antenna is used to detect its orthogonal polarization components of the polarization-modulated THz radiation simultaneously, the ratio of *p*- and *s*-polarized components of THz radiation reflected from samples is measured with a high precision, giving rise to the ellipsometric information on the samples.

5. Summary

We fabricated and evaluated two new types of PC antennas. One of which was the Schottky PC antenna, which rectified the THz PC current and give rise to a signal proportional to the THz radiation intensity. The main advantage of this PC antenna is the detection of the THz radiation intensity without the time-delay scan required for the ordinary PC antenna. The Schottky PC antenna is useful for THz sensing applications, where the spectroscopic information is not important but quick measurement of pulsed THz radiation intensity is required. The other one is the four-contact PC antenna, which is possible to generate orthogonally polarized THz radiation. With the use of total reflection Si prism it is also possible to generate the right- and left-circularly polarized THz radiation. Rotating the bias on the PC antenna by 90° , the polarization state of the emitted

THz radiation can be modulated. Such a polarization modulator is useful for polarization sensitive THz spectroscopy, such as the THz ellipsometry and THz-VCD spectroscopy.

Acknowledgements

We would like to thank Dr. Tadataka Edamura with Central Research Laboratory, Hamamatsu Photonics K. K. for his help in fabrication of LT-GaAs substrates and PC antennas.

This work was supported by the Grant-in-Aid for the Scientific Research (B) (subject # 17360030) and the Exploratory Research (subject # 16656029) programs from the Ministry of Education, Culture, Sports, Science and Technology of Japan (MEXT).

References

- [1] D. H. Auston, K. P. Cheung, and P. R. Smith: "Picosecond photoconducting Hertzian dipoles," *Appl. Phys. Lett.*, **45**, 284 (1984).
- [2] See, for example, the section 5.4 of *Classical Electromagnetic Radiation* by G. S. Smith (Cambridge University Press, 1997).
- [3] M. Tani, K. Sakai, H. Abe, S. Nakashima, H. Harima, M. Hangyo, Y. Tokuda, K. Kanamoto, Y. Abe, N. Tsukada, "Spectroscopic Characterization of Low-Temperature Grown GaAs Epitaxial Films," *Jpn. J. Appl. Phys.* **33**, 4807 (1994).
- [4] An exception is the dispersive Fourier transform spectroscopy, where the sample is inserted in one of the two beam paths of the interferometer. However, this spectroscopic method is not popular since the alignment of the two beam path in the dispersive interferometer, which must be exactly the same, is difficult to obtain a reliable dispersion spectra.
- [5] M. Tani, S. Matsuura, and K. Sakai, "Emission characteristics of photoconductive antennas based on low-temperature-grown GaAs and semi-insulating GaAs," *Appl. Opt.* **36**, 7853 (1997).
- [6] M. Tani, M. Herrmann and K. Sakai, "Generation and detection of terahertz Pulsed Radiation and its application to imaging," *Meas. Sci. Technol.* **13**, 1739 (2002).
- [7] M. Tani, O. Morikawa, S. Matsuura and M. Hangyo, "Generation of terahertz radiation by photomixing with dual- and multiple-mode lasers," *Semicond. Sci. Technol.* **20**, S151 (2005).
- [8] S. Nishizawa, K. Sakai, M. Hangyo, T. Nagashima, M. W. Takeda, K. Tominaga, A. Oka, K. Tanaka, and O. Morikawa, Chap. "Terahertz Time-Domain Spectroscopy," in *Terahertz Optoelectronics* (Ed. K. Sakai, Springer 2005).
- [9] D. T. Hodges and M. McColl, "Extension of the Schottky barrier detector to 70 μm (4.3 THz) using submicron-dimensional contacts," *Appl. Phys. Lett.*, **30**, 5 (1977).

- [10] C. Que, M. Tani, M. Hangyo, F. Miyamaru, and S. Tanaka, "Rectification of terahertz signal using a Schottky photoconductive antenna," submitted to *Appl. Phys. Lett.*
- [11] Y. Hirota, R. Hattori, M. Tani and M. Hangyo, "Polarization modulation of terahertz waves by four-contact photoconductive antenna," submitted to *Optics Express*.
- [12] Q. Chen and X.-C. Zhang, "Polarization modulation in optoelectronic generation and detection of terahertz beams," *Appl. Phys. Lett.* **74**, 3435 (1999).
- [13] R. Shimano, H. Nishimura and T. Sato, "Frequency Tunable Circular Polarization Control of Terahertz Radiation," *Jpn. J. Appl. Phys.* **44**, L676 (2005).
- [14] E. Castro-Camus, J. Lloyd-Hughes, M. B. Johnston, M. D. Fraser, H. H. Tan, and C. Jagadish, "Polarization-sensitive terahertz detection by multicontact photoconductive receivers," *Appl. Phys. Lett.* **86**, 254102 (2005).
- [15] T. Nagashima, and M. Hangyo, "Measurement of Complex Optical Constants of Highly-Doped Si Wafer Using Terahertz Ellipsometry," *Appl. Phys. Lett.*, **79**, 3917 (2001).